bioRxiv preprint doi: https://doi.org/10.1101/2025.03.20.644249; this version posted March 31, 2025. The copyright holder for this preprint (which was not certified by peer review) is the author/funder, who has granted bioRxiv a license to display the preprint in perpetuity. It is made available under aCC-BY-NC-ND 4.0 International license.

The Origin of the Ionic-strength Dependent Reentrant Behavior in Liquid-Liquid Phase Separation of Neutral IDPs

Sayantan Mondal *and* Eugene Shakhnovich*

Department of Chemistry and Chemical Biology, Harvard University
12 Oxford St. Cambridge MA 02138, U.S.A.

*Corresponding author's email: shakhnovich@chemistry.harvard.edu

Abstract: The effect of salt on coacervation of synthetic or biological polyelectrolytes is well-studied. However, recent experiments showed that largely neutral IDPs like FUS also undergo LLPS at physiological salt concentrations, dissolve at higher salt concentration and again phase separate at higher salt concentrations such as, $[C_{ion}]$~3M. Here we use analytical theory and simulations to reveal the mechanism of these transitions. At low $[C_{ion}]$, the ionic solution acts as a highly correlated medium conferring long-range effective attractive interactions between spatially distant FUS monomers. In this regime the ion concentration inside the condensate is higher than in the bulk solution. As $[C_{ion}]$ increases, the correlation length in the ionic plasma decreases, and the condensate dissolves. Second LLPS at high $[C_{ion}]$ is due to the entropy-driven crowding, and ion concentration inside the condensate is lower than in the bulk. Our study unravels a general physical mechanism of salt-dependent reentrant behavior in LLPS in neutral IDPs.

bioRxiv preprint doi: https://doi.org/10.1101/2025.03.20.644249; this version posted March 31, 2025. The copyright holder for this preprint (which was not certified by peer review) is the author/funder, who has granted bioRxiv a license to display the preprint in perpetuity. It is made available under aCC-BY-NC-ND 4.0 International license.

Introduction

Intrinsically disordered proteins (IDPs) and genetic materials can undergo liquid-liquid phase separation (LLPS) which leads to the formation of biomolecular condensates.[1] The condensates exhibit liquid droplet-like behavior and underlie the formation of membrane-less organelles (such as nucleolus, stress granules, Cajal bodies, etc.). These organelles provide an additional means to compartmentalize subcellular processes.[2] In addition to the intracellular compartmentalization, such condensates/droplets are involved in a variety of biological processes, such as genome reorganization and transcription,[3-5] stress response,[6] noise buffering,[7] signal transduction,[8] and membrane remodeling.[9,10] Disruptions in LLPS have been connected to the onset of numerous diseases, such as neurodegenerative conditions and cancer.[11] During the past decade, there has been an increasing interest in understanding the formation, microscopic structure, and kinetics of LLPS, both experimentally and theoretically.[12-19]

Over the years, the molecular grammar of LLPS has been decoded.[20,21] Although new insights into the molecular grammar are emerging, it is well-accepted that individually weak but multivalent interactions between IDPs (such as, $\pi - \pi$ stacking, cation-π, dipole-dipole, and charge-charge) are the major drivers of LLPS.[22,23] The condensation of IDPs are often favored by thermodynamics where the enthalpic gain through the formation of several weak multivalent interactions and entropic gain from the release of bound water/counterions surpasses the conformational entropy loss of the IDP and the de-mixing entropy loss.[24-26] From a surface free energy perspective, one might presume that the phase separated IDPs would eventually form a single (nearly) spherical phase. However, experiments always reveal

bioRxiv preprint doi: https://doi.org/10.1101/2025.03.20.644249; this version posted March 31, 2025. The copyright holder for this preprint (which was not certified by peer review) is the author/funder, who has granted bioRxiv a license to display the preprint in perpetuity. It is made available under aCC-BY-NC-ND 4.0 International license.

a rather poly-dispersed multi droplet state that has recently been explained theoretically from a kinetics perspective.[19] The droplet size distribution was shown to obey a power law.[27]

The LLPS propensity of an IDP is governed by its sequence and patterning of charges including phosphorylation sites.[16,18,28-30] Other than the sequence determinants, several physicochemical factors such as, temperature, presence co-solutes, ionic strength, pH, etc. can alter the LLPS propensity. In some cases, an interesting phenomenon called '*reentrant phase separation*' is observed, where the monotonic variation of a control parameter (say, ionic strength) transforms a system from a phase separated state to a macroscopically identical/similar phase separated state via two distinct transitions.[31]

The RNA-binding protein FUsed in Sarcoma (FUS) undergoes LLPS via homotypic interactions. FUS is found to be enriched in the nucleus and plays several important regulatory roles. The phase diagram of FUS condensation in the temperature-concentration space is known.[32] In a recent study, Krainer *et al*. showed that FUS (along with four other IDPs) exhibits reentrant phase separation with respect to the salt concentration in solution.[33] FUS and other IDPs show LLPS at low (physiologically relevant) as well as at high (physiologically irrelevant) salt concentrations but dissolve at intermediate salt concentrations. They suggested that, at low salt concentration regime, phase separation is driven by a mixture of hydrophobic and electrostatic interactions whereas, at high salt concentration regime, phase separation is driven by hydrophobic as well as enhanced non-ionic interactions. While their analysis provides a microscopic insight into the dominant interactions at various solvent conditions, the physical reason behind multiple reentrant transitions in a broad range of salt concentrations remain unclear. Previous studies

bioRxiv preprint doi: https://doi.org/10.1101/2025.03.20.644249; this version posted March 31, 2025. The copyright holder for this preprint (which was not certified by peer review) is the author/funder, who has granted bioRxiv a license to display the preprint in perpetuity. It is made available under aCC-BY-NC-ND 4.0 International license.

highlighted the importance of salt in phase behavior of charged polymers, polyelectrolytes and polyampholytes, including IDPs.[34-38] All these studies offered an intuitive and mechanistic explanation of the effect of salt on complexation (coacervation) of charged polymers: salt/ions screen repulsion between monomers of the charged polymer leading to coacervation. In the same vein at higher salt concentration screening becomes less effective and reentrant transition into the dilute phase ensues. However, this explanation is not applicable to mostly neutral IDPs such as FUS and TDP-43 which also show salt-dependent reentrant LLPS.[33] Thus, the mechanism of salt-dependent LLPS of a *neutral* IDP remains unresolved.

Here we use analytical statistical mechanical theory combined with explicit ion/solvent coarse-grained (CG) simulations to unravel the physical origin of the reentrant LLPS in FUS and other neutral IDPs. In the first part of the paper, we present the detailed theoretical analysis based on the modified Voorn-Overbeek approximation[21] to treat FUS polymer in complex water salt solutions. Statistical mechanical analysis predicts two reentrant LLPS transitions in a range of salt concentrations as observed in experiments as well as the distribution of ions inside and outside of the LLPS droplet in each LLPS regime. Next, we validate the findings from the analytical theory with long-timescale coarse-grained simulations that explicitly take ions and water molecules into account and discern the essential mechanism(s) by running a series of control simulations where some factors (e.g. remaining FUS charges or salt ion charges) are abrogated one by one. Overall, by using these two complementary approaches, we arrive at a general explanation of the reentrant LLPS

bioRxiv preprint doi: https://doi.org/10.1101/2025.03.20.644249; this version posted March 31, 2025. The copyright holder for this preprint (which was not certified by peer review) is the author/funder, who has granted bioRxiv a license to display the preprint in perpetuity. It is made available under aCC-BY-NC-ND 4.0 International license.

phenomenon in neutral IDPs. Although primarily motivated by the LLPS of FUS, the framework can be extended to other IDPs with a low number of charged amino acid residues.

Theoretical Analysis and Predictions

Consider the phase-separated solution of an IDP (for example, FUS) which we model as a homopolymer. The dense phase occupies a volume V (together with water and ions) and the remaining volume $(V_0 - V)$ is occupied by the dilute phase. We use the Voorn–Overbeek (VO)[35] approximation to describe thermodynamics of neutral polymer in the Flory Huggins approximation and charged salt ions in the Debye Huckel approximation with a modification to account for direct *non-electrostatic* interaction between uncharged FUS and salt ions (see Eq. S6 in the Supplementary text and accompanying discussion).

The ion-equilibrium between the condensate and the bulk is achieved at equal chemical potentials of ions in the condensate and the bulk:

$$T\ln\left(\frac{\phi_I^{in}}{\phi_I^{out}}\right) - T\ln\left(\frac{1-\phi_I^{in}-\phi_F^{in}}{1-\phi_I^{out}-\phi_F^{out}}\right) + \mu_{DH}(\phi_I^{in}) - \mu_{DH}(\phi_I^{out}) + \tilde{\chi}_{Fi}(\phi_F^{in} - \phi_F^{out}) = 0 \quad (1)$$

Where ϕ denoted volume fraction of ions and FUS inside the condensate or outside as indicated by subscript/superscript and where the DH chemical potential μ_{DH} can be written as:[39]

$$\mu_{DH}(\phi_I^{in,out}) = -\frac{Cz^2e^2}{2D}\left(\frac{\kappa}{1+\kappa b}\right) \simeq -\frac{Cz^2e^2}{2D}\sqrt{\frac{2F^2}{D\varepsilon_0 RT}I} = -A\sqrt{\phi_I^{in,out}} \quad (2)$$

In **Eq.(2)**, I is the ionic strength of the salt solution, D is the dielectric permittivity of water, F is Faraday's constant ($= eN_A$), b is effective ion size, and κ is the Debye length. At low to moderate salt concentrations $\kappa b \ll 1$ and we disregard this term.

bioRxiv preprint doi: https://doi.org/10.1101/2025.03.20.644249; this version posted March 31, 2025. The copyright holder for this preprint (which was not certified by peer review) is the author/funder, who has granted bioRxiv a license to display the preprint in perpetuity. It is made available under aCC-BY-NC-ND 4.0 International license.

Equivalently the condition of equilibrium between FUS molecules in the bulk and condensate is that chemical potential of FUS molecules in the condensate is equal to that in the bulk $\mu_F^{in} = \mu_F^{out}$ which brings in the equation that determines the volume fraction of FUS in the condensate at a fixed volume fraction of FUS in the bulk:

$$\frac{1}{L}T\ln\left(\frac{\phi_F^{in}}{\phi_F^{out}}\right) - T\ln\left(\frac{1-\phi_F^{in}-\phi_I^{in}}{1-\phi_F^{out}-\phi_I^{out}}\right) + \tilde{\chi}_{FI}\left(\phi_I^{in}-\phi_I^{out}\right) + 2\tilde{\chi}_{FF}\left(\phi_F^{in}-\phi_F^{out}\right) = 0 \quad (3)$$

Where volume fractions of ions in the bulk and the condensate are determined by the equilibrium condition **Eq. (1)**.

Now we explore the whole range of densities for all components. To that end, in **Figure 1b** we plot **Eq. (1)** for the difference of chemical potentials, $\Delta\mu_I$ *of ions* between condensed and dilute phases as a function of volume fraction of ions inside the condensate ϕ_I^{in} at various values of volume fractions of ions outside the condensate ϕ_I^{out} . For the sake of illustration, we fix the volume fraction of FUS in the dilute phase, ϕ_F^{out} at 0.1 and inside the condensate, ϕ_F^{in} at 0.3 (other values give qualitatively similar results).

bioRxiv preprint doi: https://doi.org/10.1101/2025.03.20.644249; this version posted March 31, 2025. The copyright holder for this preprint (which was not certified by peer review) is the author/funder, who has granted bioRxiv a license to display the preprint in perpetuity. It is made available under aCC-BY-NC-ND 4.0 International license.

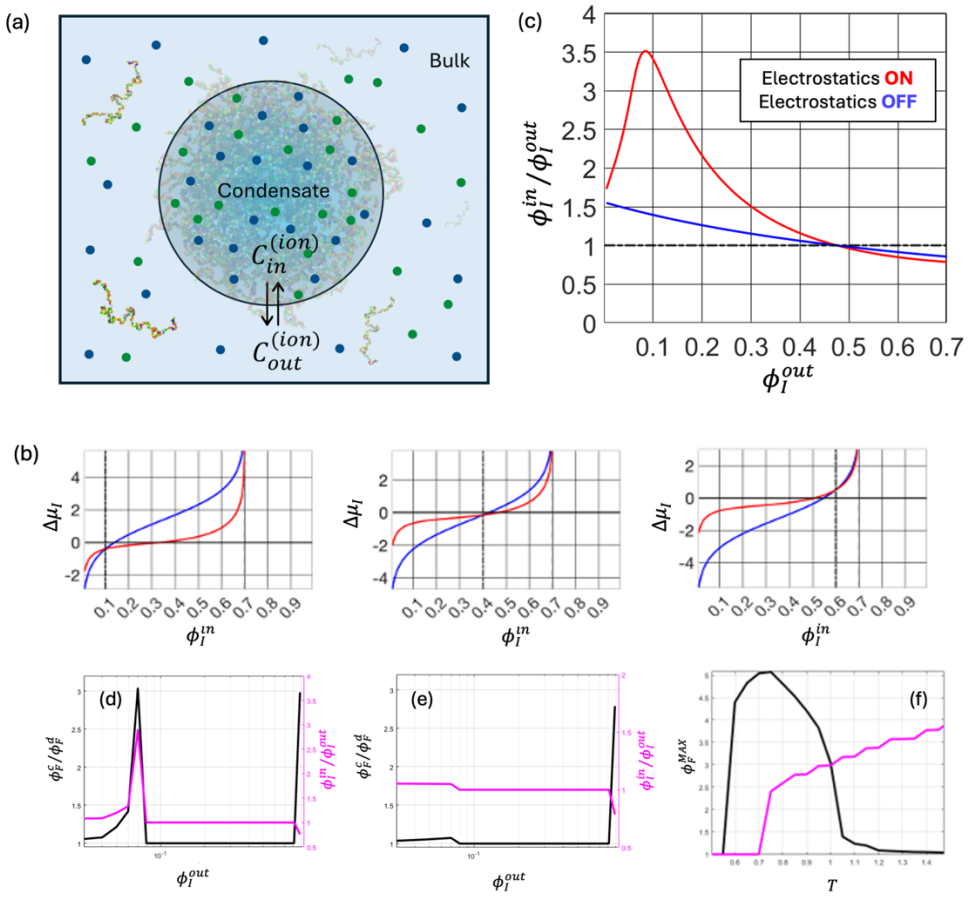

Figure 1. Statistical mechanics of liquid-liquid phase separation of neutral polymers in water salt solutions: (a) *A schematic illustration of the liquid-liquid phase separated system. The IDP rich phase is the condensate with volume fraction of ions* ϕ_I^{in} *and the dilute/bulk phase with volume fraction* ϕ_I^{out}. ***(b)*** *Graphic solution of Eq.*(1) *for the difference of chemical potential of ions in the condensed phase vs. the bulk as a function of volume fraction of salt inside the condensate (*ϕ_I^{in}*). Three panels correspond to different values of* ϕ_I^{out} *as marked by vertical dashed lines (0.1, 0.4, and 0.6 respectively) Red lines correspond to full free energy functional with electrostatics between ions while the blue lines is a control where charges are "turned off", i.e. A=0. The values of* ϕ_I^{in} *at which the lines intersect y=0 correspond to the solutions of Eq.*(1) *for* ϕ_I^{in}. ***(c)*** *Relative volume fraction of salt inside the condensate vs that in the dilute phase representing solution of Eq.4 in full range of volume fractions of salt.* ***(d)*** *Reentrant transitions in the solution of FUS. At low salt concentration FUS first condenses and as salt concentration increases condensates dissolve back into a one phase solution. Enrichment of salt inside the condensate drives the first transition until second phase*

bioRxiv preprint doi: https://doi.org/10.1101/2025.03.20.644249; this version posted March 31, 2025. The copyright holder for this preprint (which was not certified by peer review) is the author/funder, who has granted bioRxiv a license to display the preprint in perpetuity. It is made available under aCC-BY-NC-ND 4.0 International license.

separation transition accompanied by depletion of salt in the condensate. The Black curve shows the volume fraction of FUS in the condensate relative to dilute phase. The Magenta curve shows the volume fraction of ions in the condensate relative to the dilute phase. ***(e)*** *same as* ***(d)*** *but with ion charges off (A=0).* ***(f)*** *Temperature dependence of the volume fraction in the FUS condensate in the low salt phase (black lines) and the high salt phase (magenta).*

We see from **Figure 1b** that when salt concentration in the bulk is low, the condensate strongly absorbs ions and the effect is largely due to the Debye-Huckel correlation as cancellation of the DH energy in the free energy functional, **Eq.(2)** greatly diminishes absorption of ions in the condensate (blue curve). However, as the bulk salt concentration increases, this effect diminishes and finally reverses whereby the ions are depleted inside FUS condensate compared to the bulk. This can be summarized in **Figure 1c** that shows the dependence of ion concentration inside FUS condensate on the ion concentration in the bulk at fixed density of FUS condensate. We note the non-monotonic dependence of concentration of the ions with full charge interactions inside the condensate (red line). In contrast, in the absence of the DH contribution to free energy the non-monotonic dependence disappears. Rather a much weaker monotonic dependence is observed (blue line in **Figure 1c**). For further analysis of the ion equilibrium including the limits on the reentrant behavior see the **Supporting Information** text.

Finally, we solve **Eq.(1)** and **Eq.(3)** at a fixed volume fraction of FUS in the dilute phase and obtain equilibrium density (volume fraction) of FUS in the condensate in a broad range of bulk ion concentrations. The resulting typical plot (**Figure 1d**) indeed shows reentrance and second transition at a higher concentration of ions exactly as observed in experiments.[26] As an important control we explore a hypothetical situation where ions charges are

bioRxiv preprint doi: https://doi.org/10.1101/2025.03.20.644249; this version posted March 31, 2025. The copyright holder for this preprint (which was not certified by peer review) is the author/funder, who has granted bioRxiv a license to display the preprint in perpetuity. It is made available under aCC-BY-NC-ND 4.0 International license.

abrogated [A=0 in **Eqs. (1)-(3)**]. As seen on **Figure 1e** the reentrant LLPS transition at low salt concentration disappears while the transition at higher salt remains unaffected.

Finally, to get a deeper insight into the origin of the low and high salt transitions we explore temperature dependence of both (**Figure 1f**). As can be seen clearly, a lower concentration of salt at low temperatures only the first reentrant transition occurs but the second transition at high salt appears at higher temperature and becomes stronger as temperature increases while the low salt transition becomes weaker and finally disappears as temperature increases. At intermediate temperatures both transitions occur in their respective ranges of salt concentration. From that we conclude that first transition is driven by energetics of FUS-ion and ion-ion interactions and is opposed by unfavorable entropy of redistributing of ions inside/outside the condensate while second transition is clearly driven by entropy that favors more uniform distributions of all components of the complex solution inside the condensate at high salt concentrations.

In summary, the predictions from analytical theory are:

1) The reentrant transition at low ionic strengths is driven by ionic charges whereby FUS monomers effectively interact through the medium of highly correlated salt ions. In this regime ion concentration inside the condensate exceeds that of the bulk solution.
2) At a higher ionic strength charge correlations become short-range and FUS condensate dissolves.
3) At even higher (non-physiological) ionic strengths another FUS condensation transition, driven by entropy of mixing, occurs. In this regime ionic charges do not play a crucial role,

bioRxiv preprint doi: https://doi.org/10.1101/2025.03.20.644249; this version posted March 31, 2025. The copyright holder for this preprint (which was not certified by peer review) is the author/funder, who has granted bioRxiv a license to display the preprint in perpetuity. It is made available under aCC-BY-NC-ND 4.0 International license.

and the solvent components redistribute in the opposite direction, making concentration of ions inside the condensate lower than in the bulk. This transition is akin to collapse transition in a mixed solvent studied in *Ref.* 56 by Xia *et al*.

The detailed steps and descriptions of the analytical theory can be found in the **Supporting Information**. Now we turn to coarse-grained simulations with explicit solvent including water molecules, salt ions and counterions to test these predictions of analytical theory.

Materials and Methods

The conformational space of an IDP, such as FUS-LCD (163 residues long) is vast. Hence, molecular dynamics simulations at atomistic resolution are computationally expensive and far from probing the biologically relevant length- and timescales. Therefore, several coarse-graining strategies have emerged over the years. Here, we use the MARTINI v3.0[40] general purpose coarse-grained (CG) force field to model our system and test the results from the analytical theory. We choose the MARTINI model due to its recent success in understanding IDP dynamics and LLPS.[9,41-46] In addition, MARTINI has an explicit representation of the ions and water molecules (missing in other implicit solvent CG force fields) that are essential to the present study as discussed in the previous section. Below we outline the technical details and simulation protocols.

First, we create the structure from the sequence of human FUS low-complexity domain (FUS-LCD, residues 1-163) available in UniProt[47] database (ID: P35637) by using PyMOL.[48] Then the atomistic coordinates are converted into the MARTINI CG model with the

bioRxiv preprint doi: https://doi.org/10.1101/2025.03.20.644249; this version posted March 31, 2025. The copyright holder for this preprint (which was not certified by peer review) is the author/funder, who has granted bioRxiv a license to display the preprint in perpetuity. It is made available under aCC-BY-NC-ND 4.0 International license.

help of the martinize2[49] code. We randomly insert 42 copies of FUS-LCD chains inside a cubic box of dimension $(30\ nm)^3$. Following that we add the required number of counterions (2 Na^+ for each FUS chain) and excess ions (Na^+ and Cl^-) to maintain electrostatic neutrality as well as to maintain the desired ionic strength in the range of 0.0 M to 3.0 M. We note that one MARTINI water bead is equivalent to 4 molecules of water.

After a steepest descent energy minimization, we equilibrate each system for 10 ns followed by a 5 μs production run. We discard the first 2 μs from each trajectory and analyze the remaining 3 μs of the trajectory. The systems that exhibit LLPS formed a well-defined droplet within 1μs whereas systems with no LLPS propensity remained dispersed throughout. Here we use slightly recalibrated force field parameters by increasing the protein-water Lennard-Jones interaction strength (ε_{PW}) with a scaling factor $\lambda = 1.03$ that gives a reasonable transfer free-energy of FUS from the dilute to the dense phase.

For equilibration and production run, we propagate the simulations with a timestep of 10 fs and 20 fs, respectively, using the leap-from integrator. We use the modified Berendsen (V-rescale)[50] thermostat (T=298 K and τ_T=1 ps^{-1}) and the Parrinello-Rahman[51] barostat with isotropic pressure coupling (p=1 bar and τ_P = 12 ps^{-1}) to maintain an NpT ensemble. For equilibration purposes, we use the Berendsen barostat[46] with τ_P = 6 ps^{-1}. The electrostatic interactions are screened with a dielectric constant (ε_r) of 15 within and van der Waals interactions are terminated at 1.1 nm with the Verlet cut-off scheme. We perform all the simulations using GROMACS 2023.1 simulation package[52] and conduct analyses with plumed 2.5.3.[53] For visualizing the trajectories and creating snapshots, we use the visual molecular dynamics software (VMD 1.9.3).[54]

bioRxiv preprint doi: https://doi.org/10.1101/2025.03.20.644249; this version posted March 31, 2025. The copyright holder for this preprint (which was not certified by peer review) is the author/funder, who has granted bioRxiv a license to display the preprint in perpetuity. It is made available under aCC-BY-NC-ND 4.0 International license.

For the potential of mean force (PMF) calculations between two FUS monomers, we use well-tempered metadymaics,[55] WT-MetaD (T=300K and BiasFactor=5.0) with the inter center-of-mass distance (r_{COM}) as the collective variable (**Figure 5a**, inset). We solvate two FUS chains in a 30 nm cubic box with MARTINI water and ions. We set the MetaD hill width to be 0.35 nm and the initial hill height to be 1.0 kJ/mol. The MetaD hills are deposited every 1 ps and the MetaD simulations are run for 5 μs. We use PLUMED (v 2.9.0)[53] patched with GROMACS,[52] to perform the MetaD simulations and subsequent analyses.

To quantify the extent of LLPS, we calculate a contact order parameter (COP), $Q(t)$ as shown in **Eq. (4)**. The COP at a particular timeframe, t is expressed as:

$$Q(t) = \sum_{i,j} q_{ij}(t), \; and$$
$$q_{ij}(t) = \frac{1 - \left(r_{ij}(t) / r_0 \right)^6}{1 - \left(r_{ij}(t) / r_0 \right)^{12}} \tag{4}$$

where $r_{ij}(t)$ is the distance between the ith and jth beads at time t and r_0 is fixed to be 0.5 nm. Hence, $q_{ij}(t)$ can vary smoothly from 1 to 0 for a given pair. We further define ΔQ as the gain in COP by subtracting the time-averaged COP for FUS with only counterion system (**Figure 3d**), Q_0. Therefore, $\Delta Q = \langle Q(t) \rangle - Q_0$. The pair-interaction energies are obtained using '*gmx energy*' code. The energies contain both Lennard-Jones and electrostatic interactions.

Results

First, we study the propensity of FUS to undergo LLPS in the range of ion concentrations from 0.0 M to 3.0 M as predicted theoretically and observed in experiment.[33] We observe no condensation at 0 M. Starting from physiological 0.15 M salt FUS undergoes

bioRxiv preprint doi: https://doi.org/10.1101/2025.03.20.644249; this version posted March 31, 2025. The copyright holder for this preprint (which was not certified by peer review) is the author/funder, who has granted bioRxiv a license to display the preprint in perpetuity. It is made available under aCC-BY-NC-ND 4.0 International license.

LLPS into single compact cluster which dissolves beyond 1.0 M NaCl. Interestingly, LLPS reappears when salt concentration is above 2.5 M. (**Figure 2a**) This 'extremely high' salt concentration regime, although biologically non-relevant, is important to understand from a physics perspective as noted above.

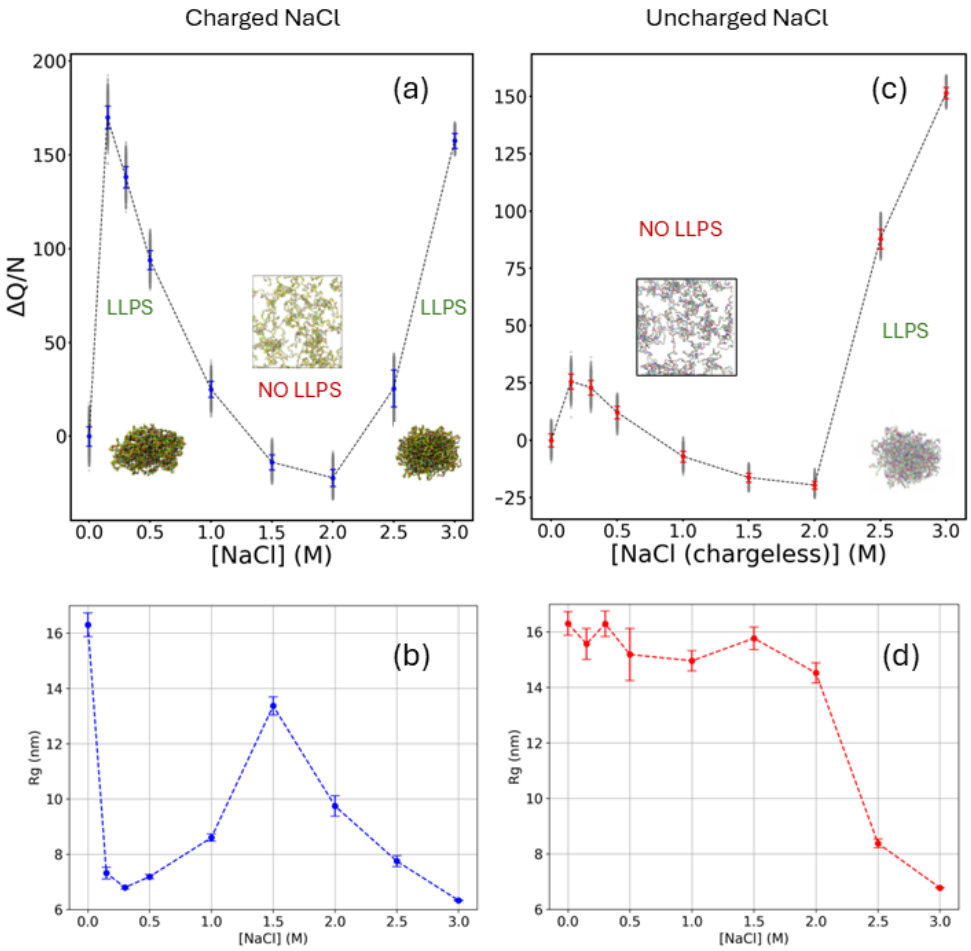

Figure 2. Time-averaged contact order parameter (ΔQ) per FUS chain against the ionic strength of the solution: *(a) when sodium and chloride ions retain their charges and (c) when the sodium and chloride ions are made chargeless LJ beads. An increase in ΔQ/N above a threshold indicates condensation.* ***Time averaged radius of gyration, Rg against the ionic strength of the solution:*** *(b) when sodium and chloride ions retain their charges and (d) when the sodium and chloride ions are made chargeless LJ beads. A decrease in Rg*

bioRxiv preprint doi: https://doi.org/10.1101/2025.03.20.644249; this version posted March 31, 2025. The copyright holder for this preprint (which was not certified by peer review) is the author/funder, who has granted bioRxiv a license to display the preprint in perpetuity. It is made available under aCC-BY-NC-ND 4.0 International license.

indicates condensation. Both (a) and (b) panels show the 'double reentrant' phenomena. The dotted lines should be used as guides to the eye.

In **Figure 2a**, we plot the density of FUS $\Delta Q/N$ against salt concentration, [NaCl]. A sharp increase can be observed from [NaCl]=0.0 M to 0.15 M. The value of $\Delta Q/N$ decreases upon further increase of salt concentration and the LLPS cluster fully dissolves when [NaCl] exceeds 1.0 M. However, when [NaCl] > 2.0 M the value of $\Delta Q/N$ increases again and reaches the values observed at 0.15 M [NaCl]. This is the second entrance into the 'LLPS' regime from the 'no LLPS' zone. Therefore, we observe the double reentrant transition where the second reentrance is observed as in experiments.[33] From the error bars (or, standard deviations) **Figure 2a**, important information regarding the dynamics of the condensates can be gleaned. Although condensation/LLPS occurs at around [NaCl]=0.15 M and at around [NaCl]=3.0 M, the condensate is more dynamic for [NaCl]=0.15 M system (more dispersed data) whereas, at [NaCl]=3.0 M the condensate is less fluctuating (less dispersed data). The same can also be gleaned from another order parameter, radius of gyration (Rg) of all the FUS chains, shown in **Figure 2b**. Rg sharply decreases for [NaCl]~0.15M-0.50M followed by an increase around [NaCl]~1.0 M and again decrease at higher [NaCl].

In **Figure 2c** we plot the same quantity as in **Figure 2a** (that is, $\Delta Q/N$ vs [NaCl]), however for an artificial control system with uncharged salt (essentially LJ beads). This is equivalent to 'turning off' the electrostatic interactions in the analytical approach. There is a slight increase in $\Delta Q/N$ at lower salt concentrations, but without condensation. The absence of condensation can be understood from the high Rg values at that salt concentration (**Figure 2d**) and from visual inspections. Interestingly, FUS undergoes LLPS at high salt (here,

bioRxiv preprint doi: https://doi.org/10.1101/2025.03.20.644249; this version posted March 31, 2025. The copyright holder for this preprint (which was not certified by peer review) is the author/funder, who has granted bioRxiv a license to display the preprint in perpetuity. It is made available under aCC-BY-NC-ND 4.0 International license.

LJ bead) concentration, indicated by a sharp increase in $\Delta Q/N$ (**Figure 2c**) and a decrease in Rg (**Figure 2d**). The analytical theory also predicted that the system would undergo phase separation at high salt concentrations when electrostatic interactions are 'turned off' (**Figure 2e**). Plots for pairwise interaction energies against salt concentrations, namely E_{FUS}, $E_{FUS-Ion}$, E_{FUS-W}, and E_{Ion} can be found in **Supporting Information** (**Figures S1** and **S2**).

Next, we explore in detail the mechanism of LLPS of FUS including, crucially, the role of ions. For control and comparison, we study several model systems with the same box size and number of FUS molecules. The five systems are as follows: (1) Original model of FUS at 0.15 M NaCl, (2) artificial 'chargeless' FUS chains in 0.15 M NaCl where charges of FUS chains are abrogated, (3) FUS with artificial 'chargeless' 0.15 M NaCl whereby charges of salt ions are set to zero, (4) FUS with only few Na^+ ions serving as counterions to FUS charges, and (5) FUS with only 0.15 M Na+ ions without any Cl^- ions. The last system contains high amount of net positive charge. Below we detail the rationale behing studying these systems.

The purpose of the control system-2 is to check whether the 4 charges on FUS (N-ter, C-ter, Asp-5, and Asp-46) assist the LLPS in any way. It turns out that FUS whose own charges are set to 0 forms condensate in the regular NaCl solution whose salt ion charges are intact (**Figure 3b**). Therefore, we can rule out the role of FUS counterion mediated inter-polymeric interaction in the FUS LLPS. The purpose of system-3 is to test whether the ionic charges are required for LLPS in the low [NaCl] regime as predcited by the analytical theory. In agreement with the theoretical predcition, the condensate does not form in this case (**Figure 3c**). The purpose of the control system 4 (**Figure 3d**) is to demonstrate that FUS, with only its counterions (that is, 2 Na^+ ions per chain) cannot exhibit LLPS. Importantly in control system

bioRxiv preprint doi: https://doi.org/10.1101/2025.03.20.644249; this version posted March 31, 2025. The copyright holder for this preprint (which was not certified by peer review) is the author/funder, who has granted bioRxiv a license to display the preprint in perpetuity. It is made available under aCC-BY-NC-ND 4.0 International license.

5 (**Figure 3e**), where Na^+ ions retained their positive charges and the Cl anions were absent, the highly correlated Debye-Huckel plasma does not exist and FUS did not form condensate. This supports the conclusion from the analytical theory that LLPS at low salt concentration is driven by the interactions throgh highly correlated ionic medium. All in all we conclude that highly correlated system of opopsitely charged ions – a Debye Huckel plasma – is driving reentrant condensation and dissolution of FUS at low [NaCl]. This mechanism has significant similarity to polymer-salt-induced condensation of DNA or psi(ψ)-condensation,[56,57] discussed subsequently.

bioRxiv preprint doi: https://doi.org/10.1101/2025.03.20.644249; this version posted March 31, 2025. The copyright holder for this preprint (which was not certified by peer review) is the author/funder, who has granted bioRxiv a license to display the preprint in perpetuity. It is made available under aCC-BY-NC-ND 4.0 International license.

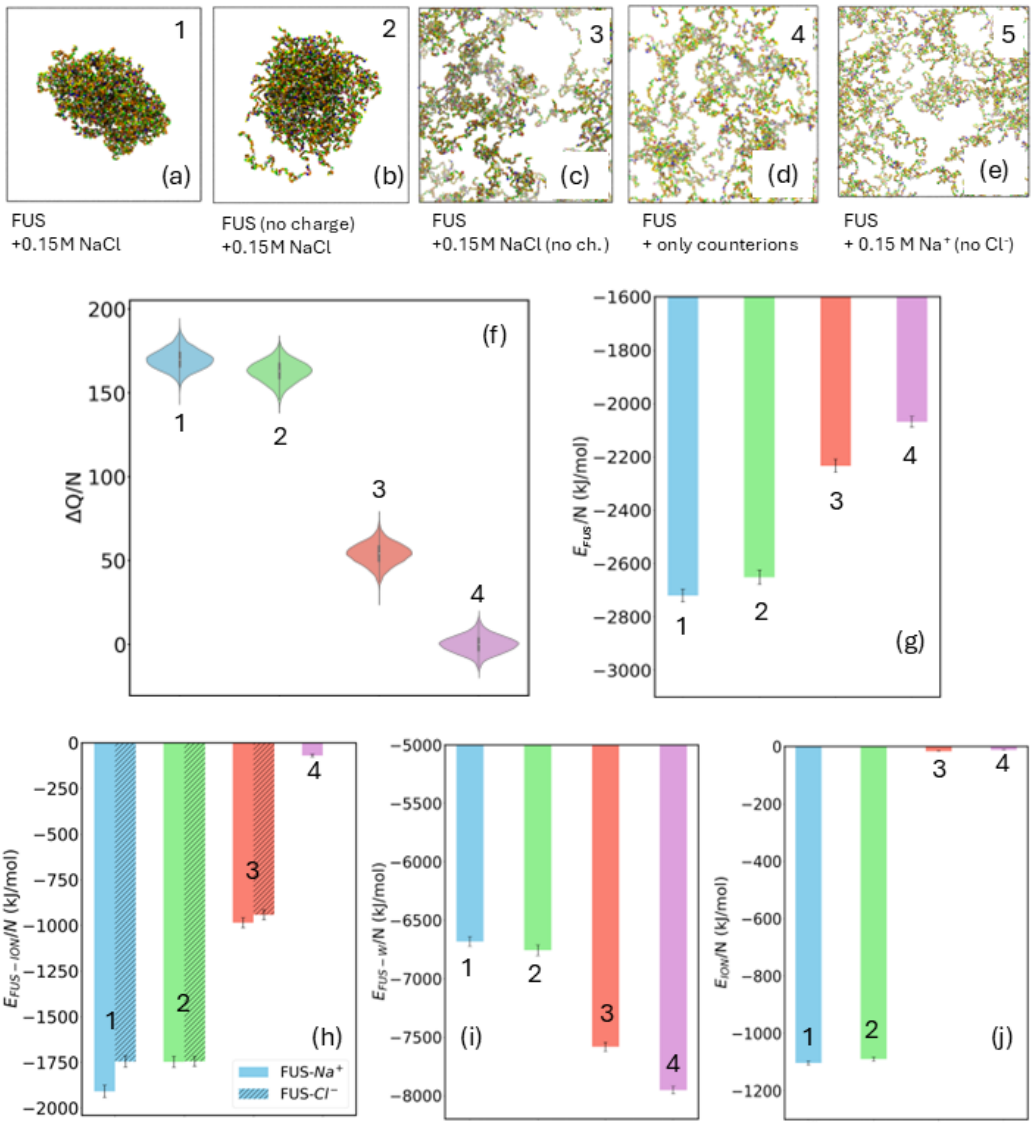

Figure 3. Representative snapshots and pair-interaction energetics from coarse-grained molecular dynamics: *(a) FUS chains in 0.15M NaCl shows condensate formation, (b) Artificial FUS chains with no charges in in 0.15M NaCl shows condensate formation, (c) FUS chains in 0.15M artificial NaCl with no charges (which behave like LJ beads) shows no condensate formation, (d) FUS with only Na^+ (2 ions per chain to maintain electrostatic neutrality) ions shows no condensate formation, and (e) FUS with 0.15 M excess Na^+ (no Cl^-) ions shows no condensate formation. The first four systems are respectively denoted as 1,2,3, and 4 in the subsequent plots. (f) Variation of the contact order parameter (ΔQ) per FUS chain for the four systems. Time-averaged interaction energies of different pairs: (g)*

bioRxiv preprint doi: https://doi.org/10.1101/2025.03.20.644249; this version posted March 31, 2025. The copyright holder for this preprint (which was not certified by peer review) is the author/funder, who has granted bioRxiv a license to display the preprint in perpetuity. It is made available under aCC-BY-NC-ND 4.0 International license.

Among FUS chains, (h) Between FUS and ions, (i) Between FUS and water beads, and (j) Among the ions.

To quantify the extent of LLPS, in **Figure 3f** we plot ΔQ normalized by the number of FUS chains for the four systems depicted in **Figure 3a** through **Figure 3d**. For systems 1 and 2, the gain in number of contact pairs is at the maximum. On the contrary, for systems 3 and 4, the value of $\Delta Q/N$ is much lower. Note that these are not the absolute values mentioned in the **Methods** section. In **Figure 3g** we show the time-averaged pair interaction energies (LJ + Coulomb) between FUS chains, E_{FUS}/N. As one can presume, the interaction between FUS chains is the strongest for system 1, and almost comparable for system 2. However, these energies are substantially lower for systems 3 and 4, where the interaction primarily arises due to intra-chain contacts. In **Figure 3h**, the energies of FUS-ion interaction are plotted, separately for Na^+ and Cl^-. The values for systems 1 and 2 are lower which indicate enhanced interaction of FUS with salt ions. The FUS chains of system 1 interact slightly stronger with the Na^+ than with the Cl^- owing to the presence of two negatively charged aspartate residues in each chain. Such distinction is not present in system 2 where FUS is made chargeless. In system 3, the excess ions are chargeless but the counterions (2 Na^+ per chain) are not. Hence, it shows enhanced interaction with Na^+, but the values are almost 50% reduced. System-4 has no Cl^- and only Na^+ counterions. A reverse trend is observed in **Figure 3i** where the energy of FUS with water are plotted. Systems 1 and 2 interact less with water compared to system 3 and 4. **Figure 3j** shows the interaction between energies of ions. Here we find that ions interact favorably when LLPS occurs. Overall, from the pair-energetics we find that LLPS of FUS stabilizes the inter-FUS, FUS-ion, and inter-ionic interactions; and destabilizes

bioRxiv preprint doi: https://doi.org/10.1101/2025.03.20.644249; this version posted March 31, 2025. The copyright holder for this preprint (which was not certified by peer review) is the author/funder, who has granted bioRxiv a license to display the preprint in perpetuity. It is made available under aCC-BY-NC-ND 4.0 International license.

the FUS-water interactions. These results are consistent with the theoretical prediction that interaction between ions of the salt drive LLPS of FUS at low [NaCl].

Next, we test the prediction from the analytical theory about spatial distribution of ions, that is, in LLPS occurring at low salt concentrations the condensate will absorb more ions, and in the second LLPS occurring at higher concentrations the condensate will expel ions (**Figure 1b-Figure 1d**). Our CG simulations essentially exhibit the same behavior as presented in **Figure 4**. For the condensate at [NaCl]=0.15 M, there is a significantly increased population of both Na^+ and Cl^- ions in the interior of the FUS condensate, as seen from the representative simulation snapshots (**Figure 4a**, **Figure 4b**, and **Figure 4c**). In **Figure 4d**, **Figure 4e**, and **Figure 4f** we respectively plot the spatial density profile of FUS, sodium, and chloride along the X-dimension of the simulation box. The density profile clearly shows the excessive adsorption of ions by the FUS condensates. In the high salt concentration LLPS regime, for [NaCl]=3.0 M, the opposite effect is observed where the FUS-rich region of the box has lower density of ions than the region outside the condensate. It can be seen in the snapshots (**Figure 4g**, **Figure 4h**, and **Figure 4i**) and also from the density profile plots (**Figure 4j**, **Figure 4k**, and **Figure 4l**). This shows moderate expulsion of ions from the interior after reentrance. Also note that excessive adsorption of ions in the low salt regime is much stronger than their expulsion in the high salt regime (almost 3-fold for adsorption and ~15% for expulsion) in agreement with the predictions of the analytical theory as highlighted in **Figure 1.**

bioRxiv preprint doi: https://doi.org/10.1101/2025.03.20.644249; this version posted March 31, 2025. The copyright holder for this preprint (which was not certified by peer review) is the author/funder, who has granted bioRxiv a license to display the preprint in perpetuity. It is made available under aCC-BY-NC-ND 4.0 International license.

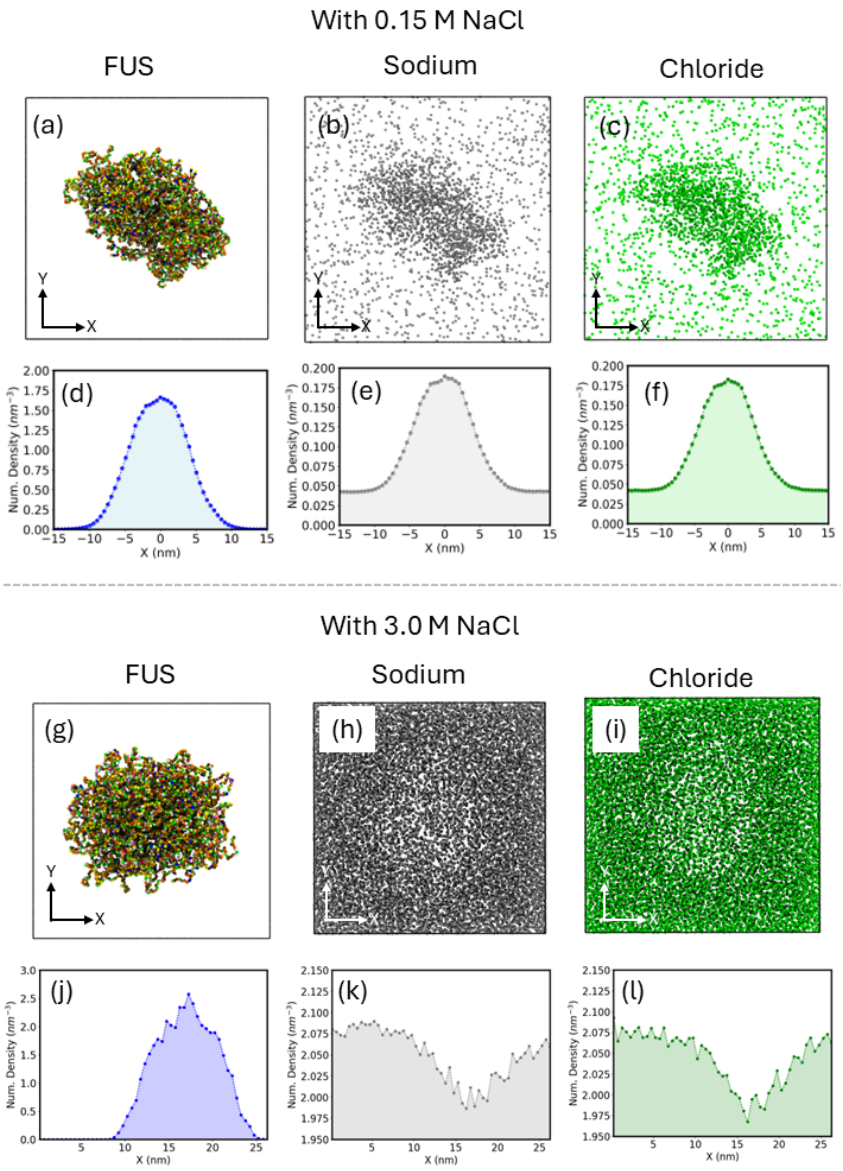

Figure 4. Spatial distribution of the FUS condensate, sodium, and chloride ions inside the simulation box for two different ionic strengths*, namely, 0.15 M and 3.0 M. In the low ion concentration regime, the density of ions follows the density of FUS as shown pictorially in panels (a) – (c) and quantitatively from the spatial density profiles in panels (d) - (e). On the contrary, in the high ionic concentration regime, the FUS condensate expels ions from its interior as shown pictorially in panels (g) – (i) and quantitatively from the spatial density profiles in panels (j) – (l).*

From the WT-MetaD calculations we obtain the PMF between two FUS-LCD chains in 0.15 M NaCl solution, with and without the ionic charges. The resultant PMFs are shown in

bioRxiv preprint doi: https://doi.org/10.1101/2025.03.20.644249; this version posted March 31, 2025. The copyright holder for this preprint (which was not certified by peer review) is the author/funder, who has granted bioRxiv a license to display the preprint in perpetuity. It is made available under aCC-BY-NC-ND 4.0 International license.

Figure 5a where the blue trace shows an effective attraction between two FUS chains when electrostatics are 'on', with approximately 30 kJ/mol free energy stabilization in the associated state. In the same figure, the red trace shows an effective repulsion between the FUS chains when electrostatics are 'off'. This demonstrates the long-ranged effective attraction through the ionic media. A detailed discussion on this can be found in the following section.

Discussion

Studies of charged polymers (polyelectrolytes and polyampholytes) in solutions containing salts have a long history.[34-36,58-61] Discovery of membrane-less organelles in living cells formed by IDPs undergoing LLPS[26] reignited interest in biopolymer condensates in physiologically relevant environments.[62] Statistical mechanical analysis using field-theoretical tools from polymer theory[63,64] provided detailed phase diagrams for specific IDPs enriched in charged amino acids.[37] In these cases, salts affect the phase state of a polyelectrolyte by screening electrostatic repulsion between its charges giving rise, in some cases, to LLPS. In a similar vein, coacervation of polyelectrolytes of opposite charges appeared to be strongly salt-dependent as electrostatics is a driving force in these situations.[59]

However recent experiments showed that largely neutral IDPs such as FUS undergo a set of complex reentrant transitions in a broad range of salt concentration.[33] The authors of [33] carried out a series of atomistic simulations to demonstrate that different forces are dominant at different salt concentrations. While insightful these studies do not provide a

bioRxiv preprint doi: https://doi.org/10.1101/2025.03.20.644249; this version posted March 31, 2025. The copyright holder for this preprint (which was not certified by peer review) is the author/funder, who has granted bioRxiv a license to display the preprint in perpetuity. It is made available under aCC-BY-NC-ND 4.0 International license.

clear mechanistic explanation of the multiple transitions that FUS and other neutral IDPs undergo in a broad range of salt concentrations with multiple instances of reentrance.

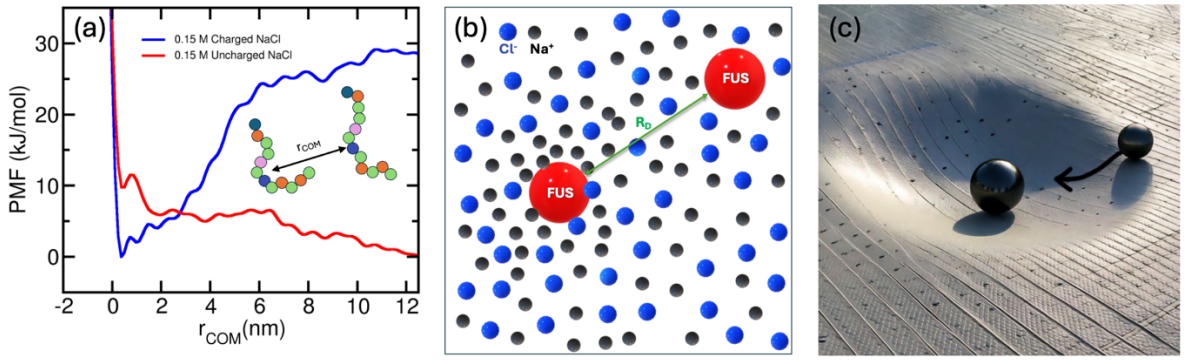

Figure 5. Effective attraction between FUS monomers through highly correlated medium of salt ions*: (a) Potential of mean force between two FUS chains calculated by using well-tempered metadynamics. The two FUS chains are attractive in 0.15 M NaCl solution but becomes repulsive when the ionic charges are set to '0', that is, electrostatics are turned off. (b) Illustration of the attractive LJ interaction between a FUS monomer (red sphere) and ions creates a local increase of density around the FUS monomer that propagates at the correlation length that is Debye radius, R_d. Effective density gradient creates an energetic "funnel" that is felt by another FUS monomers creating long-range attraction between them. As salt concentration increases the Debye length decreases, and the attraction weakens leading to dissolution of condensates. (c) A schematic depiction of the mechanism by which a perturbation of the ion plasma by attractive short range LJ interaction with a FUS monomer creates local density increase near the FUS monomer which propagates up to the scale of correlation length in the ion plasma (which coincides with Debye radius, R_d) and creates effective potential well for another FUS monomer which is attracted to the "density bump" via short range LJ interaction potential between FUS and ions.*

Here, we use a combination of theoretical and computational approaches to reach mechanistic understanding of the physics of complex reentrant phase behavior of neutral IDPs such as FUS at different salt concentrations. At low salt concentrations interaction between a FUS monomer and a salt ion perturbs density of highly correlated salt ions creating a density gradient that extends up to Debye length. Given that interactions between

bioRxiv preprint doi: https://doi.org/10.1101/2025.03.20.644249; this version posted March 31, 2025. The copyright holder for this preprint (which was not certified by peer review) is the author/funder, who has granted bioRxiv a license to display the preprint in perpetuity. It is made available under aCC-BY-NC-ND 4.0 International license.

ions and FUS monomers are energetically favorable due to LJ attraction the ion density gradient created by one FUS monomer serves as an effective energetic funnel creating a long range attractive potential for another FUS monomer(s), as schematically shown in **Figure 5a** and **Figure 5b**. This physical mechanism is validated in our CG simulations.

We carried out a set of control simulations by adding one energetic contribution at a time and checking how it affects LLPS. To check whether the marginal charges of FUS (two Aspartate and the N- and C- termini) and corresponding counterions matter we removed these charges and observed no difference. However, when we removed the charges of salt ions, the LLPS at low salt concentration disappeared. To assess the role of long-range correlation in ionic plasma, we created an artificial solvent where only salt anions were present and again found no LLPS in that case, these observations from simulations support the notion that the medium of strongly correlated ionic plasma is crucial for LLPS of neutral FUS at physiological salt concentrations. Remarkably, the same control calculations in the analytical theory (e.g. dropping the DH free energy of ion interactions from the free energy functional in **Eq.2**) lead to the same outcome as in simulations: disappearance of the LLPS at physiological salt (**Figure 1e**). Interestingly both simulations and theory show a miniscule increase of FUS density at physiological concentration in a control system where ion charges are removed (**Figure 1e** and **Figure 2b**) demonstrating a remarkable agreement between theory and simulations.

This mechanism is conceptually similar to polymer-salt-induced condensation, often referred to as ψ-condensation.[57] ψ-condensation refers to collapse of DNA in the presence of a neutral polymer (PEO) and monovalent salt in solution.[65] In ψ-condensation, DNA-

bioRxiv preprint doi: https://doi.org/10.1101/2025.03.20.644249; this version posted March 31, 2025. The copyright holder for this preprint (which was not certified by peer review) is the author/funder, who has granted bioRxiv a license to display the preprint in perpetuity. It is made available under aCC-BY-NC-ND 4.0 International license.

induced perturbation of density of PEO propagates at longer scales due to correlated fluctuations in polymer solution creating an effective long range potential well for DNA[57] – a mechanism similar to the one described here where the role of correlated medium is played by ions.

As salt concentration increases beyond physiological levels, screening effects become increasingly significant, leading to a suppression of long-range attractive interactions and, ultimately, dissolution of the condensate. This is consistent with the classical understanding of LLPS in charged systems, where the introduction of excess salt reduces electrostatic cohesion, promoting mixing with the bulk. Our results show that this dissolution occurs around between 1 M – 2 M salt concentration. However, an intriguing phenomenon emerges at even higher ionic strengths, where LLPS reappears beyond 2M salt concentration, marking the second reentrant transition. Unlike the condensation mechanism at low salt, phase separation in this regime is not driven by FUS-salt interactions but rather by an ion-exclusion mechanism. The FUS condensate expels ions from its interior, allowing the system to regain phase separation despite the high salt environment. The second LLPS transition at high salt concentration is an entropy driven phenomenon which disappears at low temperature as predicted by the theory (see **Figure 1e**). CG simulations show the same behavior: while transition at low salt is crucially dependent on ion charges the second transition at high salt is insensitive to the abrogation of charges of salt ions suggesting that it is driven mainly by LJ energy of association between FUS and salt and, crucially entropy of all components in the condensate.[56]

bioRxiv preprint doi: https://doi.org/10.1101/2025.03.20.644249; this version posted March 31, 2025. The copyright holder for this preprint (which was not certified by peer review) is the author/funder, who has granted bioRxiv a license to display the preprint in perpetuity. It is made available under aCC-BY-NC-ND 4.0 International license.

This is a striking departure from the behavior observed at low ionic strength, underscoring the nontrivial role of electrostatic correlations and entropic forces in governing phase behavior in IDPs with a low fraction of charged residues. A key insight from our study is that the mechanism of LLPS at low and high salt concentrations is fundamentally distinct, even though both regimes exhibit phase separation. This distinction is evident in the differences in ion distribution, pair interaction energies, and overall condensate morphology. The ψ-condensation-like mechanism at physiological salt concentrations leads to a system where ions are deeply embedded in the condensate, while at extreme salt conditions, the driving force shifts towards an entropically favorable phase separation driven by ion exclusion. These findings not only provide a microscopic understanding of the reentrant LLPS of FUS but also suggest a generalizable framework for other IDPs with low charge density.

Overall, our study provides a comprehensive statistical mechanical view of mechanisms of LLPS in water-salt solutions where theoretical predictions are tested and verified by molecular simulations. By unraveling the mechanistic details of LLPS across different ionic environments, we not only explain recent experimental observations but also establish a broader paradigm for understanding phase separation in biologically relevant systems.

Acknowledgements

This work is supported by the National Institute of Health (Grant R35 GM139571). SM and ES thank the 'Faculty of Arts and Science Research Computing' (FASRC) at Harvard University for computational resources.

bioRxiv preprint doi: https://doi.org/10.1101/2025.03.20.644249; this version posted March 31, 2025. The copyright holder for this preprint (which was not certified by peer review) is the author/funder, who has granted bioRxiv a license to display the preprint in perpetuity. It is made available under aCC-BY-NC-ND 4.0 International license.

References

1 Hyman, A. A., Weber, C. A. & Jülicher, F. Liquid-liquid phase separation in biology. *Annu. Rev. Cell Dev. Biol* **30**, 39-58 (2014).

2 Banani, S. F., Lee, H. O., Hyman, A. A. & Rosen, M. K. Biomolecular condensates: organizers of cellular biochemistry. *Nature reviews Molecular cell biology* **18**, 285-298 (2017).

3 Ladouceur, A.-M. *et al*. Clusters of bacterial RNA polymerase are biomolecular condensates that assemble through liquid–liquid phase separation. *Proceedings of the National Academy of Sciences* **117**, 18540-18549 (2020).

4 Laflamme, G. & Mekhail, K. Biomolecular condensates as arbiters of biochemical reactions inside the nucleus. *Communications Biology* **3**, 773-773 (2020).

5 Gibson, B. A. *et al*. Organization of chromatin by intrinsic and regulated phase separation. *Cell* **179**, 470-484 (2019).

6 Guillén-Boixet, J. *et al*. RNA-induced conformational switching and clustering of G3BP drive stress granule assembly by condensation. *Cell* **181**, 346-361 (2020).

7 Klosin, A. *et al*. Phase separation provides a mechanism to reduce noise in cells. *Science* **367**, 464-468 (2020).

8 Case, L. B., Ditlev, J. A. & Rosen, M. K. Regulation of transmembrane signaling by phase separation. *Annual review of biophysics* **48**, 465-494 (2019).

9 Mondal, S. & Cui, Q. Coacervation-Induced Remodeling of Nanovesicles. *Journal of Physical Chemistry Letters* (2023). https://doi.org/10.1021/acs.jpclett.3c00705

10 Mangiarotti, A., Chen, N., Zhao, Z., Lipowsky, R. & Dimova, R. Wetting and complex remodeling of membranes by biomolecular condensates. *Nature Communications* **14**, 2809-2809 (2023).

11 Alberti, S. & Dormann, D. Liquid–liquid phase separation in disease. *Annual review of genetics* **53**, 171-194 (2019).

12 Pak, C. W. *et al*. Sequence determinants of intracellular phase separation by complex coacervation of a disordered protein. *Molecular cell* **63**, 72-85 (2016).

13 Abyzov, A., Blackledge, M. & Zweckstetter, M. Conformational dynamics of intrinsically disordered proteins regulate biomolecular condensate chemistry. *Chemical Reviews* **122**, 6719-6748 (2022).

14 Dinic, J., Marciel, A. B. & Tirrell, M. V. Polyampholyte physics: Liquid–liquid phase separation and biological condensates. *Current opinion in colloid & interface science* **54**, 101457-101457 (2021).

15 Kaur, T. *et al*. Sequence-encoded and composition-dependent protein-RNA interactions control multiphasic condensate morphologies. *Nature communications* **12**, 872-872 (2021).

16 McCarty, J., Delaney, K. T., Danielsen, S. P. O., Fredrickson, G. H. & Shea, J.-E. Complete phase diagram for liquid–liquid phase separation of intrinsically disordered proteins. *The journal of physical chemistry letters* **10**, 1644-1652 (2019).

17 Ranganathan, S. & Shakhnovich, E. I. Dynamic metastable long-living droplets formed by sticker-spacer proteins. *Elife* **9**, e56159-e56159 (2020).

bioRxiv preprint doi: https://doi.org/10.1101/2025.03.20.644249; this version posted March 31, 2025. The copyright holder for this preprint (which was not certified by peer review) is the author/funder, who has granted bioRxiv a license to display the preprint in perpetuity. It is made available under aCC-BY-NC-ND 4.0 International license.

18 Ranganathan, S., Dasmeh, P., Furniss, S. & Shakhnovich, E. Phosphorylation sites are evolutionary checkpoints against liquid–solid transition in protein condensates. *Proceedings of the National Academy of Sciences* **120**, e2215828120-e2215828120 (2023).

19 Chattaraj, A. & Shakhnovich, E. I. Separation of sticker-spacer energetics governs the coalescence of metastable condensates. *Biophysical Journal* (2025).

20 Wang, J. *et al*. A molecular grammar governing the driving forces for phase separation of prion-like RNA binding proteins. *Cell* **174**, 688-699 (2018).

21 Saar, K. L. *et al*. Learning the molecular grammar of protein condensates from sequence determinants and embeddings. *Proceedings of the National Academy of Sciences* **118**, e2019053118-e2019053118 (2021).

22 Brangwynne, C. P., Tompa, P. & Pappu, R. V. Polymer physics of intracellular phase transitions. *Nature Physics* **11**, 899-904 (2015).

23 Li, P. *et al*. Phase transitions in the assembly of multivalent signalling proteins. *Nature* **483**, 336-340 (2012).

24 Ahlers, J. *et al*. The key role of solvent in condensation: Mapping water in liquid-liquid phase-separated FUS. *Biophysical journal* **120**, 1266-1275 (2021).

25 Mukherjee, S. & Schäfer, L. V. Thermodynamic forces from protein and water govern condensate formation of an intrinsically disordered protein domain. *Nature Communications* **14**, 5892-5892 (2023).

26 Berry, J., Brangwynne, C. P. & Haataja, M. Physical principles of intracellular organization via active and passive phase transitions. *Reports on Progress in Physics* **81**, 046601-046601 (2018).

27 Lee, D. S. W. *et al*. Size distributions of intracellular condensates reflect competition between coalescence and nucleation. *Nature Physics* **19**, 586-596 (2023).

28 Das, R. K. & Pappu, R. V. Conformations of intrinsically disordered proteins are influenced by linear sequence distributions of oppositely charged residues. *Proceedings of the National Academy of Sciences* **110**, 13392-13397 (2013).

29 Monahan, Z. *et al*. Phosphorylation of the FUS low-complexity domain disrupts phase separation, aggregation, and toxicity. *The EMBO journal* **36**, 2951-2967 (2017).

30 Rumyantsev, A. M., Johner, A. & de Pablo, J. J. Sequence blockiness controls the structure of polyampholyte necklaces. *ACS Macro Letters* **10**, 1048-1054 (2021).

31 Narayanan, T. & Kumar, A. Reentrant phase transitions in multicomponent liquid mixtures. *Physics Reports* **249**, 135-218 (1994).

32 Dignon, G. L., Zheng, W., Kim, Y. C., Best, R. B. & Mittal, J. Sequence determinants of protein phase behavior from a coarse-grained model. *PLoS computational biology* **14**, e1005941-e1005941 (2018).

33 Krainer, G. *et al*. (2021).

34 Srivastava, S. & Tirrell, M. V. Polyelectrolyte complexation. *Advances in chemical physics* **161**, 499-544 (2016).

35 Michaeli, I., Overbeek, J. T. G. & Voorn, M. J. Phase separation of polyelectrolyte solutions. *Journal of Polymer Science* **23**, 443-450 (1957).

36 Sing, C. E. & Perry, S. L. Recent progress in the science of complex coacervation. *Soft Matter* **16**, 2885-2914 (2020).

bioRxiv preprint doi: https://doi.org/10.1101/2025.03.20.644249; this version posted March 31, 2025. The copyright holder for this preprint (which was not certified by peer review) is the author/funder, who has granted bioRxiv a license to display the preprint in perpetuity. It is made available under aCC-BY-NC-ND 4.0 International license.

37 Lin, Y.-H. *et al*. Electrostatics of salt-dependent reentrant phase behaviors highlights diverse roles of ATP in biomolecular condensates. *eLife* **13**, RP100284-RP100284 (2025).
38 Zhang, P., Shen, K., Alsaifi, N. M. & Wang, Z.-G. Salt partitioning in complex coacervation of symmetric polyelectrolytes. *Macromolecules* **51**, 5586-5593 (2018).
39 McQuarrie, D. A. *Statistical Mechanics*. (2000).
40 Souza, P. C. T. *et al*. Martini 3: a general purpose force field for coarse-grained molecular dynamics. *Nature methods* **18**, 382-388 (2021).
41 Tsanai, M., Frederix, P. W. J. M., Schroer, C. F. E., Souza, P. C. T. & Marrink, S. J. Coacervate formation studied by explicit solvent coarse-grain molecular dynamics with the Martini model. *Chemical Science* **12**, 8521-8530 (2021).
42 Mehta, N., Mondal, S., Watson, E. T., Cui, Q. & Chapman, E. R. The juxtamembrane linker of synaptotagmin 1 regulates Ca2+ binding via liquid-liquid phase separation. *Nature Communications* **15**, 262-262 (2024).
43 Mondal, S. & Cui, Q. Sequence Sensitivity in Membrane Remodeling by Polyampholyte Condensates. *The Journal of Physical Chemistry B* **128**, 2087-2099 (2024). https://doi.org/10.1021/acs.jpcb.3c08149
44 Thomasen, F. E., Pesce, F., Roesgaard, M. A., Tesei, G. & Lindorff-Larsen, K. Improving Martini 3 for disordered and multidomain proteins. *Journal of Chemical Theory and Computation* **18**, 2033-2041 (2022).
45 Benayad, Z., von Bülow, S. r., Stelzl, L. S. & Hummer, G. Simulation of FUS protein condensates with an adapted coarse-grained model. *Journal of chemical theory and computation* **17**, 525-537 (2020).
46 Zerze, G. H. Optimizing the martini 3 force field reveals the effects of the intricate balance between protein–water interaction strength and salt concentration on biomolecular condensate formation. *Journal of Chemical Theory and Computation* **20**, 1646-1655 (2023).
47 UniProt: the universal protein knowledgebase in 2021. *Nucleic acids research* **49**, D480-D489 (2021).
48 DeLano, W. L. Pymol: An open-source molecular graphics tool. *CCP4 Newsl. Protein Crystallogr* **40**, 82-92 (2002).
49 Kroon, P. C. *et al*. Martinize2 and vermouth: Unified framework for topology generation. *arXiv preprint arXiv:2212.01191* (2022).
50 Bussi, G., Donadio, D. & Parrinello, M. Canonical sampling through velocity rescaling. *The Journal of chemical physics* **126** (2007).
51 Bernetti, M. & Bussi, G. Pressure control using stochastic cell rescaling. *The Journal of Chemical Physics* **153** (2020).
52 Abraham, M. J. *et al*. GROMACS: High performance molecular simulations through multi-level parallelism from laptops to supercomputers. *SoftwareX* **1**, 19-25 (2015).
53 Tribello, G. A., Bonomi, M., Branduardi, D., Camilloni, C. & Bussi, G. PLUMED 2: New feathers for an old bird. *Computer physics communications* **185**, 604-613 (2014).
54 Humphrey, W., Dalke, A. & Schulten, K. VMD: visual molecular dynamics. *Journal of molecular graphics* **14**, 33-38 (1996).

bioRxiv preprint doi: https://doi.org/10.1101/2025.03.20.644249; this version posted March 31, 2025. The copyright holder for this preprint (which was not certified by peer review) is the author/funder, who has granted bioRxiv a license to display the preprint in perpetuity. It is made available under aCC-BY-NC-ND 4.0 International license.

55 Barducci, A., Bussi, G. & Parrinello, M. Well-tempered metadynamics: a smoothly converging and tunable free-energy method. *Physical review letters* **100**, 020603 (2008).

56 Xia, Z., Das, P., Shakhnovich, E. I. & Zhou, R. Collapse of unfolded proteins in a mixture of denaturants. *Journal of the American Chemical Society* **134**, 18266-18274 (2012).

57 Grosberg, A. Y., Erukhimovitch, I. Y. & Shakhnovich, E. I. On the Theory of Ψ-Condensation. *Biopolymers* **21**, 2413-2432 (1982).

58 Kudlay, A. & Olvera de la Cruz, M. Precipitation of oppositely charged polyelectrolytes in salt solutions. *The Journal of chemical physics* **120**, 404-412 (2004).

59 Borue, V. Y. & Erukhimovich, I. Y. A STATISTICAL-THEORY OF WEAKLY CHARGED POLY-ELECTROLYTES - FLUCTUATIONS, EQUATION OF STATE, AND MICROPHASE SEPARATION. *Macromolecules* **21**, 3240-3249 (1988).

60 Borue, V. Y. & Erukhimovich, I. Y. A STATISTICAL-THEORY OF GLOBULAR POLYELECTROLYTE COMPLEXES. *Macromolecules* **23**, 3625-3632 (1990). https://doi.org/10.1021/ma00217a015

61 Danielsen, S. P. O., McCarty, J., Shea, J. E., Delaney, K. T. & Fredrickson, G. H. Small ion effects on self-coacervation phenomena in block polyampholytes. *J Chem Phys* **151**, 034904 (2019). https://doi.org/10.1063/1.5109045

62 Baidya, L., Maity, H. & Reddy, G. Salts Influence IDP Properties by Modulating the Population of Conformational Clusters. *The Journal of Physical Chemistry B* (2025).

63 Lin, Y.-H., Brady, J. P., Chan, H. S. & Ghosh, K. A unified analytical theory of heteropolymers for sequence-specific phase behaviors of polyelectrolytes and polyampholytes. *The Journal of chemical physics* **152** (2020).

64 Najafi, S., McCarty, J., Delaney, K. T., Fredrickson, G. H. & Shea, J. E. Field-Theoretic Simulation Method to Study the Liquid-Liquid Phase Separation of Polymers. *Methods Mol Biol* **2563**, 37-49 (2023). https://doi.org/10.1007/978-1-0716-2663-4_2

65 Lerman, L. S. A transition to a compact form of DNA in polymer solutions. *Proceedings of the National Academy of Sciences* **68**, 1886-1890 (1971).